FUDMA Journal of Sciences (FJS)
ISSN online: 2616-1370
ISSN print: 2645 - 2944
Vol. 7 No. 6, December (Special Issue), 2023, pp 362 -372
DOI: https://doi.org/10.33003/fjs-2023-0706-2214

OPTIMAL SIZING OF SOLAR-WIND HYBRID MICROGRID USING IMPROVED GREY WOLF OPTIMIZATION ALGORITHM A CASE STUDY OF KADUNA - NIGERIA

Bankole Samson Sesan, *Isiyaku Abubakar, Nasiru B. Kadandani and Isaac B. Olalekan

Department of Electrical Engineering, Bayero University Kano, PMB 3011, Kano, Nigeria

*Corresponding authors' email: iabubakar.ele@buk.edu.ng

ABSTRACT

This paper presents an improved grey wolf optimization algorithm (IGWOA) for optimal sizing of an isolated photovoltaic (PV), wind turbine (WT), and battery energy storage (BES) hybrid microgrid. To demonstrate the effectiveness of the proposed approach, atmospheric data sets comprising of wind, solar, and temperature of Kaduna International Airport were collected from Nigerian Meteorological Agency while the load demand data was collected from Kaduna International Airport Electricity Distribution Center. The microgrid optimal sizing was formulated as a constrained single objective optimization problem. Constraints including, loss of power supply probability (LPSP), power balance, generation limits and battery state of charge (SOC) were imposed. Three simulation scenarios were considered. Firstly, the target allowable maximum LPSP was fixed at 25% and the algorithm was able to determine the optimal sizing of the hybrid microgrid components and minimize the initial cost from 169,880.00 USD to 112,356.40 USD per annum resulting in 34% savings in cost. Secondly, the effect of the target allowable maximum LPSP variation was investigated, and it was found that the total installed capacity of the system decreases with increase in LPSP thereby decreasing the total cost. Additionally, a novel electricity price index (EPI) was introduced in order to quantify the degree of optimality of the solution. The EPI was found to increase exponentially with increase in LPSP, resulting in an EPI of < 0.05USD/kWh at 20% LPSP. Lastly, to validate the proposed approach, a comparative analysis between the IGWOA and other algorithms was carried out, and the proposed IGWOA proved applicable.

Keywords: Photovoltaic (PV), wind turbine (WT), battery energy storage (BES), improved grey wolf optimization algorithm (IGWOA), loss of power supply probability (LPSP)

INTRODUCTION

The conventional source of energy for power generation is mainly from fossil-fuels which is known to be the major cause of greenhouse gas emissions (GHG) and global warming. So, as the load demand is increasing, there is corresponding increase in the usage of fossil-fuels which also results to increase in GHG emissions. To counteract the process of global warming associated with fossil-fuel based energy sources, renewable energy sources such as wind can be adapted (Dan-Isa & Kadandani, 2013). Presently, there is scarcity and rapid depletion of fossil fuels worldwide in addition to the problem of global warming caused by GHG emissions. (Traoré, 2018). This rising concerns over global warming have stimulated the interest in reducing GHG emissions, especially those emitted during electricity generation from conventional sources like coal, oil, and natural gas. So, new environmental policies are being legislated to curtail GHG. For instance, 160 countries around the world have signed the Paris agreement to combat against the climate changes (unfccc.int/paris_agreement/items/9485.php, 2017). To fulfill the agreement, nations around the globe are planning to reduce their GHG emissions, e.g., Kingdom of Saudi Arabia has planned to reduce CO_2 emissions by 130 million tons per year by 2030 (Akram et. al, 2017). Thus, there is urgent need to reduce the utilization of fossil fuels by looking for suitable alternative to conventional power generation that will be reliable, sustainable, economical and eco-friendly. Also, the energy security concerns have urged nations to look for sustainable sources of energy to replace depleting fossil fuels (Traoré, 2018).

More so, the epileptic nature of power supply system and its socio-economic effects on the people in developing countries like Nigeria has become a thing of concern to all stake holders. Inadequate power supply due to insufficient power generation and regular grid system collapse in the country have crippled a lot of businesses and render a lot of people jobless especially in some major cities and major markets in Nigeria. The work reported in (Kadandani 2015) have proposed grid integration of wind farms for complementing the national grid in meeting the electricity demand. Currently, about 1.3 billion people out of the total population of 7 billion do not have access to modern energy supply (Enerdata, 2017). The International Energy Association (IEA) reported that about 622 million people out of the 1.3 billion populations do not have access to electricity in Africa (Administration, 2016). While 621 million people out of the 1.3 billion populations are from sub-Saharan Africa, only approximately 1 million people are from Africa's northern region (Ainah, 2015). The energy report further reveals that the sub-Saharan Africa has the lowest electrification access rate in the world. For instance, more than 60% of Nigeria's citizens do not have access to its national grid (Akinyele, 2016).

In addition to this, most of the world's population live in remote or rural areas, which are sporadically populated and geographically isolated. Due to the low demand, some of these areas are not connected to the grid. To develop such areas, a well-organized and financially feasible method needs to be found to provide such areas with electricity. Therefore, renewable energy sources are recommended as the most suitable alternative energy sources because they are pollution free, economical and also offer power supply solutions for remote areas not accessible by the grid supply (Mousa et. al, 2010; & Bagdanov et. al, 2021).

Renewable energy sources such as solar and wind are clean, inexhaustible, limitless, and environmental friendly (Jayachandran, 2017). Such properties have fascinated the energy sector to use renewable energy sources on a higher scale (Varetsky & Hanzelka, 2015). However, all renewable energy sources have one form of disadvantage or the other. The one that is common to wind and solar sources is their dependency on unpredictable factors such as weather and climatic conditions. Fortunately, due to complementary nature of both sources, some of these complications can be addressed by overcoming the weaknesses of one with the strengths of the other (Varetsky & Hanzelka, 2015). This brings us to the concept of hybrid micro-grid power system. Furthermore, a smooth integration of these renewable energy resources with the grid network can be achieved with the aid of solid state transformer (SST) which apart from providing voltage transformation can also provide other additional ancillary services to the grid (Kadandani, Hassan & Abubakar (2023a). Current source converter (CSC) and voltage source converter (VSC) based high voltage direct current (HVDC) transmission system can be used to transmit and connect the electricity in bulk form to stiff and weak grids respectively (Kadandani, Hassan & Abubakar (2023b).

Micro-grids comprise of low-voltage distribution systems with distributed energy sources, storage devices, and controllable loads that are operated either islanded or connected to the main power grid in a controlled and coordinated way. This new concept requires further research to ascertain its suitability and affordability in developing countries like Nigeria in order to take advantage of its numerous benefits. Therefore, this research is set out to develop an improved grey wolf optimization algorithm (IGWOA) for optimal sizing of an isolated photovoltaic (PV), wind turbine (WT), and battery energy storage (BES) based hybrid microgrid system.

The aim of this research work is to find the optimal size of PV array, WT and BES system for standalone hybrid microgrid system for rural communities using Kaduna international airport as a case study. The schematic diagram of a typical remote solar-wind hybrid microgrid system is shown in Figure 1 (Traoré, 2018).

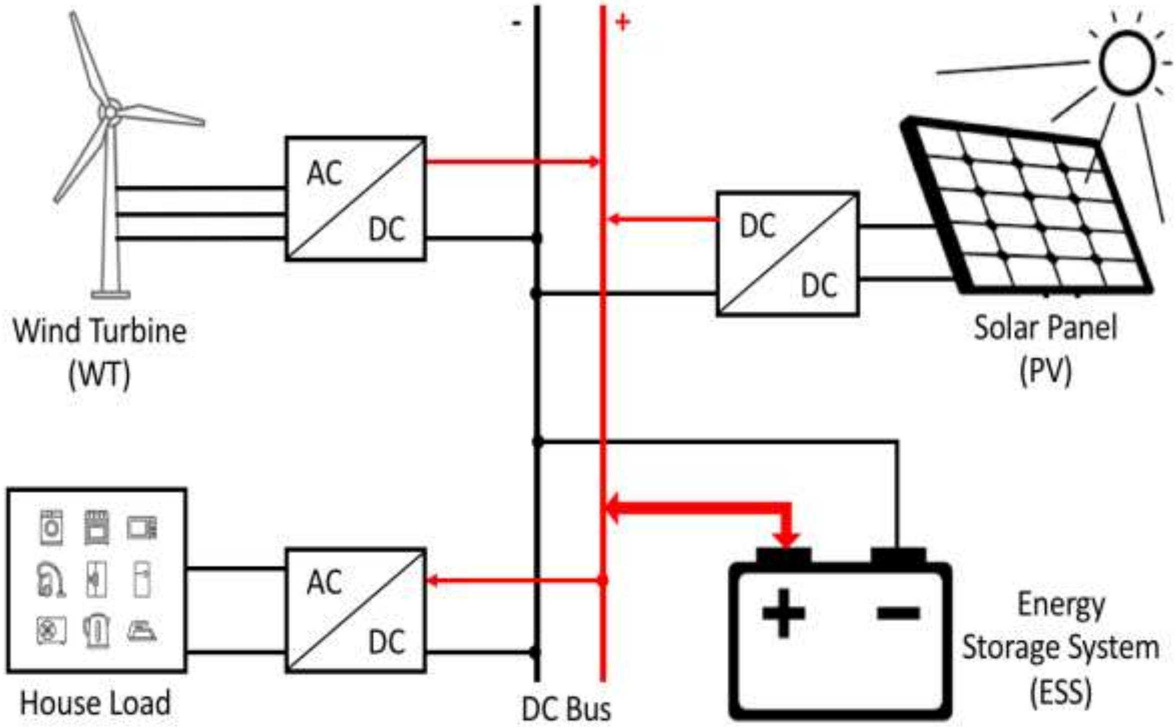

Figure 1: Schematic Diagram of Islanded Wind-Solar Hybrid Microgrid System

MATERIALS AND METHODS

Mathematical Model of the System

This subsection describes the mathematical models governing the system operation. This includes the PV model, WT model, BES system model, and the system reliability model. The models were adopted from (Traoré, 2018). However, pseudo code approach was employed for easy implementation in MATLAB environment.

Photovoltaic System Model

The output power of the PV module, the efficiency of the PV module and the cell temperature can be determined by using equations 1, 2 and 3 respectively (Traoré, 2018);

$$P_{PV}\,(t) = \mu_{PV}\,.\,A_{PV}\,.\,G(t) \quad (1)$$

$$\mu_{PV} = \mu_{STC}\,.\,\mu_{MPPT}\,\left[1 - a\,(T_c - T_{STC})\right] \quad (2)$$

$$T_c = T_a + \left[\frac{NOCT-20}{800}\right].\,G\,(t) \quad (3)$$

where A_{pv} is the area of a PV module in (m^2), $G(t)$ is the hourly total solar irradiance in (W/m), η_{pv} is the efficiency of the PV module, η_{STC} is reference efficiency of the PV cell at standard temperature condition (STC), η_{MPPT} is the efficiency of the maximum peak power tracker, T_c is the temperature of the PV cell in (˚C), T_a is the ambient temperature, T_{STC} is the reference temperature of the PV cell at STC (25˚C), NOCT is the nominal operating cell temperature and α is the temperature coefficient of the PV cell.

Wind Turbine Model

The output power from a WT at time t depends on the wind speed and can be obtained from equation (4) (Traoré, 2018);

$$P_{WT}(t) = \begin{cases} 0 & V(t) < V_{ci} \\ a.V^3(t) - b \cdot P_{WT}^r & V_{ci} \leq V(t) < V_r \\ P_{WT}^r & V_r \leq V(t) < V_{co} \\ 0 & V(t) \geq V_{co} \end{cases} \quad (4)$$

where $a = \frac{P_{WT}^r}{V_r^3 - V_{ci}^3}$; $b = \frac{V_{ci}^3}{V_r^3 - V_{ci}^3}$; $V(t)$ is the wind speed at time t in m/s; $P_{wt}^r, v_{ci}, \mathrm{v}_r$, and v_{co} represent the rated power of wind turbine, the cut-in speed, rated speed and cut-out speed respectively.

Similarly, the WT system is modelled as a wind energy conversion system (WECS) that takes-in the wind speed (v_w) as variable, and a set of constants which include, P_{wt}^r, v_{ci}, v_r, and v_{co}. The model evaluates the power output per wind turbine, which is scaled by another parameter, N_{wt}, to obtain the generated wind power P_{wt}.

Battery Energy Storage System Model

The discharging and charging energies of the BES at time t can be obtained from (5) and (6), respectively (Traoré, 2018).

$$E_{ESS}^d(t) = E_{SS}(t-1) - [E_{Load}(t) - E_{PV}(t) - E_{WT}(t)]/\mu_d \quad (5)$$

$$E_{ESS}^c(t) = E_{SS}(t-1) - [E_{PV}(t) - E_{WT}(t) - E_{Load}(t)].\mu_c \quad (6)$$

where $E_{SS}(t-1)$ is the energy at time $t-1$ in kWh E_{PV}, E_{WT}, E_{Load} are the respective energies in PV, WT and load; η_d and η_c are the discharge and charge efficiencies of the ESS, respectively.

Equations (5) and (6) can be rewritten as (7) and (8) (Traoré, 2018).

$$E_{ESS}^d(t) = E_{SS}(t-1) - P_{ESS}^d(t).\Delta t/\mu_d \quad (7)$$

$$E_{ESS}^c(t) = E_{SS}(t-1) - P_{ESS}^c(t).\Delta t/\mu_c \quad (8)$$

where $P_{ESS}^d(t) = P_{Load}(t) - P_{PV}(t) - P_{WT}(t)$ is the power discharged by the ESS; $E_{ESS}^c(t) = P_{PV}(t) - P_{WT}(t) - P_{Load}$ (t) is power charged into the ESS; and $\Delta t = 1$ since the time interval is 1 hour.

Reliability Model

A microgrid is said to be reliable if it can satisfy consumers' electricity demand at the time of need. The reliability of the system is described using the loss of power supply probability (LPSP) given by equation 9 (Traoré, 2018).

$$LPS(t) = P_{Load}(t) - [P_{PV}(t) + P_{WT}(t) + P_{ESS}^d(t)].\mu_{inv} \quad \textbf{(9)}$$

Improved Grey Wolf Optimization (IGWO) Algorithm

Grey wolf optimizer (GWO) is a population-based meta-heuristics algorithm that simulates the leadership hierarchy and hunting mechanism of grey wolves in nature as proposed by (Mirjalili, 2014). The proposed IGWO algorithm incorporates crossover and mutation into the conventional grey wolf optimization algorithm (Liu et. al 2019, Wang et. al, 2019; & Long, 2016).

Kaduna international airport situated at Afaka in Igabi local government area of Kaduna state, Nigeria (which is about 22.9km northwest of Kaduna and about 63.8km southwest of Zaria on latitude 10.6966°and longitude 7.32045°) was used as the case study for the hybrid microgrid system (HMGS). The data for wind speed, solar irradiance and ambient temperature were collected from NiMET while the load demand data was collected from Kaduna international airport electricity distribution center. The data collected were used for determining the optimal size of the HMGS components.

RESULTS AND DISCUSSION

Description of the System Set-up

The renewable resources; wind, solar and temperature data were used to simulate optimum size of the proposed HMGS to supply the load data collected from a remote area in Kaduna state, Nigeria, in order to investigate and demonstrate the effectiveness of the proposed IGWO strategy. To validate the developed models and algorithm, a validation case that serves as a comparative analysis between the IGWO and four other algorithms, namely; particle swarm optimizer (PSO); differential evolution (DE); water cycle algorithm (WCA); and the conventional grey wolf optimizer (GWO) was carried out and the results obtained are presented in Figure 2 through 7. Table 1 presents the numerical values of some of the main simulation parameters. In this work, each solution candidate was represented by a row vector of 3 elements representing N_{pv}, N_{wt}, and SOC_{max} respectively. A population of 100 solution candidates (grey wolves) was chosen. Each of the elements in the solution was bounded by [0, 1000000]. The number of iterations was fixed at 100. The mean hourly solar irradiance; wind speed; and load diversity factor of a single day was determined and used through this work. The total electrical energy demand was maintained at 2731.4kWh. The simulation scenarios and the results obtained are further described in the following sub-sections.

Table 1: Simulation Input Parameter Description

S/No.	Symbol	Description	Value	Unit
1	λ	Parameter of BESS life span	5	years
2	C_{cap}^{pv}	Capital cost of PV	0.8	US$/W
3	C_{op}^{pv}	Operational cost of PV	0.04	US$/W
4	C_{cap}^{wt}	Capital cost of WT	0.67	US$/W
5	C_{op}^{wt}	Operational cost of WT	0.1005	US$/W
6	C_{cap}^{B}	Capital cost of BESS	0.15	US$/Wh
7	C_{op}^{B}	Operational cost of BESS	0.015	US$/Wh
8	η_{stc}	Efficiency at standard test condition	15.7	%

9	η_{mppt}	Efficiency at maximum power point	65	%
10	A_{pv}	Area of PV panel	1.6236	m^2
11	P_{pv}^{r}	Rated power of a PV panel	255	W
12	T_{stc}	Temperature at standard test condition	25	^{O}C
13	NOCT	Nominal operating cell temperature	47	^{O}C
14	α	Temperature coefficient of PV panel	0.006	$1/(^{O}C)$
15	P_{wt}^{r}	Rated power of a WT	1500	W
16	v_{ci}	Cut-in wind speed	2.5	m/s
17	v_{r}	Rated wind speed	15	m/s
18	v_{co}	Cut-out wind speed	25	m/s
19	*DOD*	BESS Depth of Discharge	0.8	p.u.
20	η_{ch}	BESS charging efficiency	85	%
21	η_{dch}	BESS discharging efficiency	90	%
22	η_{inv}	Inversion efficiency of the converter	95	%
23	$P_{L}^{\max}$	Peak load	155	kW
24	sdr	BESS self-discharge rate	0.1	%

Simulation Case 1: Optimal Sizing at the Maximum Allowable LPSP

In this scenario, the maximum allowable LPSP was kept at 25%, and the IGWO algorithm was executed, with all other input parameters as specified above. Under this condition, LPSP of 20.08% was obtained. The optimum N_{pv} and N_{wt} were found to be 2113 and 252 units respectively. This corresponds to 539KW and 378KW installed capacities of PV and WT respectively while the optimum BESS capacity was found to be 386 kWh, corresponding to the maximum state of charge (SOC_{max}). The optimum cost (minimum objective function value) of the system was found to be 112,356.4 USD per annum, from an initial cost of 169,880 USD per annum, resulting in at least 34% savings in cost. Figure 2 shows the hourly generation schedule of the system. It represents daily power balance where the total power generated by the PV, WT and BES are supplied to the load but when there is excess power generation, BES is used for storage purpose.

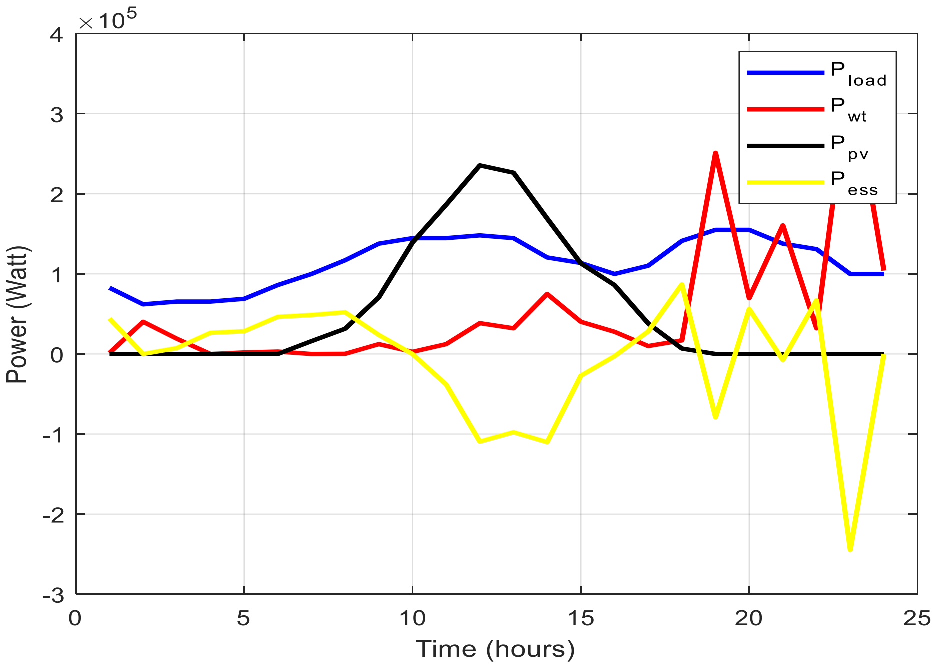

Figure 2: Mean Hourly Power Generation Optimum Schedule

Similarly, the total energy produced by the PV and WT generating system; the total energy charged and discharged by the BES; the total energy not served and the total energy consumed by the dump load are also determined over an entire day as shown in the pie chart in Figure 3.

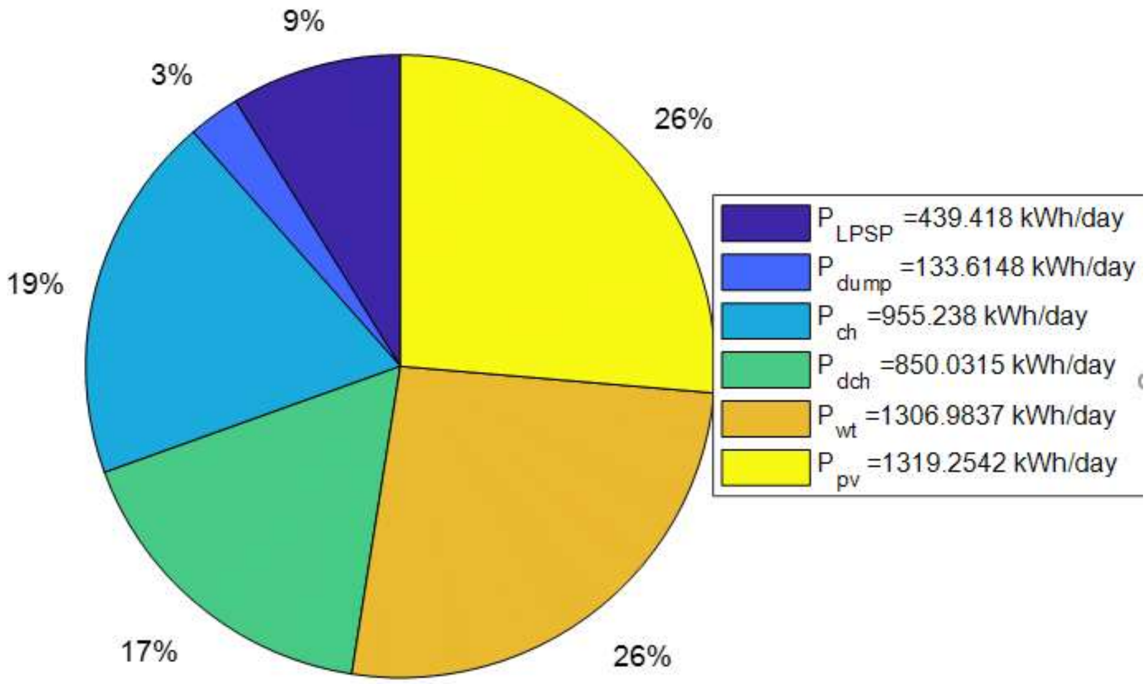

Figure 3: Energy Supply Composition by the Hybrid MG System

Simulation Case 2: The Effect of Variation in LPSP on the Total Installed Capacity of the HMGS

This case is intended to investigate the effect of LPSP on the HMGS design/sizing. This case is similar to case 1, in that all the input parameters, except the LPSP remain the same. However, the LPSP was gradually decreased between 97% and 0%, at approximately 10% interval and the results obtained are shown in Table 2. The results obtained in Table 2 are further described in figures 4 and 5 where figure 4 represents installed capacities of the HMGS components while figure 5 represents total energy production and BES losses respectively.

Table 2: Capacities, Cost and Energy Output with Varying LPSP

LPSP (%)	Cost (USD/year)	PV		WT		BESS		
		P_{PV}^{Inst} (kW)	Output (kWh)	P_{WT}^{Inst} (kW)	Output (kWh)	P_{BESS}^{Inst} (kW)	E_{BESS}^{Inst} (kWh)	Losses (kWh)
97	2467	14	33	11	36	0	0	0
88	11998	68	165	50	171	0	0	0
79	22499	144	352	83	285	0	0	0
69	36141	166	407	158	545	38	38	10
58	52180	184	452	239	825	114	114	32
48	70411	179	440	342	1183	211	211	74
39	82655	567	1393	162	560	101	322	101
28	120579	184	450	555	1919	412	648	215
19	147596	181	444	668	2308	518	897	294
8	161891	937	2303	234	809	271	1142	350
1	169880	425	1044	678	2344	527	925	384
0	162824	737	1813	465	1608	327	853	386

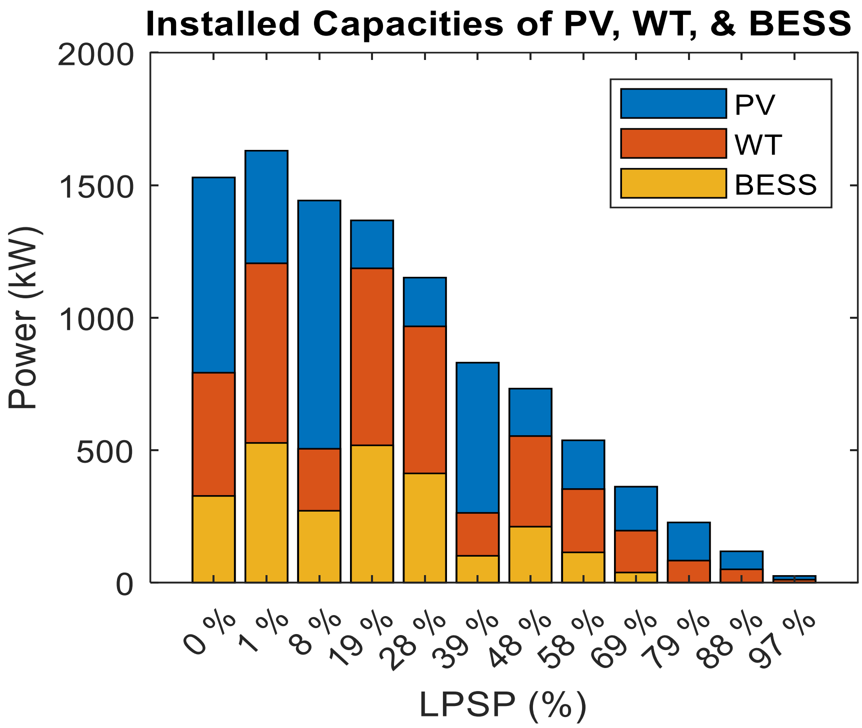

Figure 4: Installed Capacities of the PV, WT and BESS

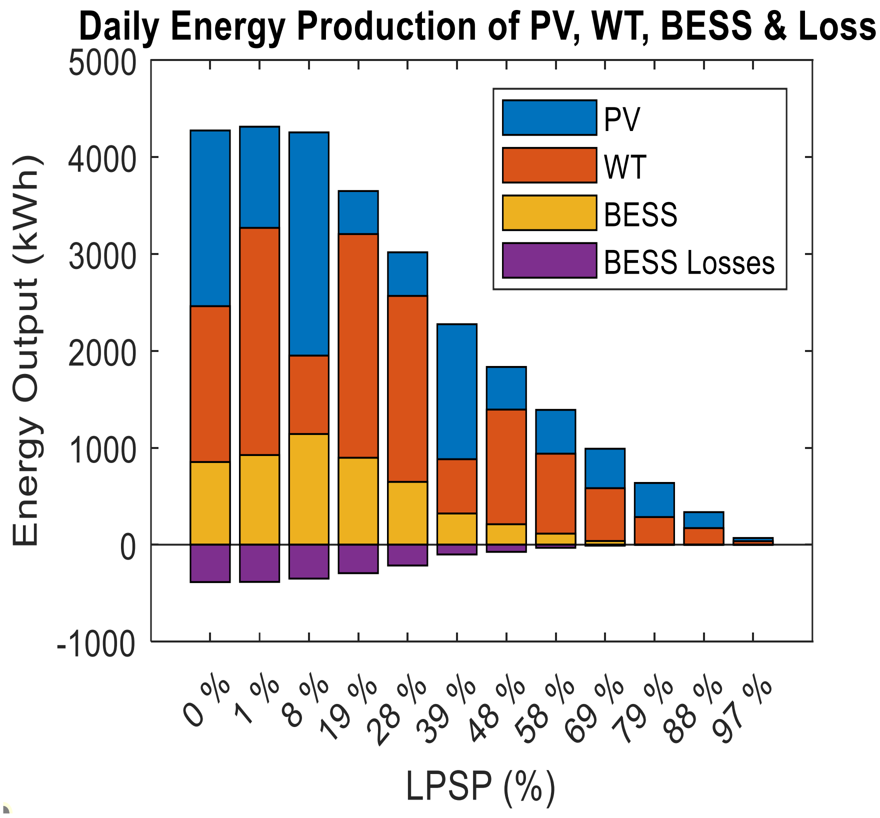

Figure 5: Total Energy Production and BESS Losses

A novel index called "electricity price index" (EPI) is proposed to quantify the degree of optimality. The value of EPI for each LPSP was computed using equation 10 and represented by Figure 6. As shown in the figure, the lower the value of EPI, the higher the degree of optimality of a given solution.

$$EPI = \frac{OF}{\left(\left(1-\frac{LPSP}{100}\right)\sum_{t=1}^{24} P_L(t)\right)\left(P_{PV}^{Inst}+P_{WT}^{Inst}+P_{BESS}^{Inst}\right)} \quad (10)$$

where P_{PV}^{Inst} , P_{WT}^{Inst} and P_{BESS}^{Inst} represents kW installed capacities of PV, WT and BES respectively,
OF represents the value of the objective function, and P_L (t) represents the instantaneous value of load demand.

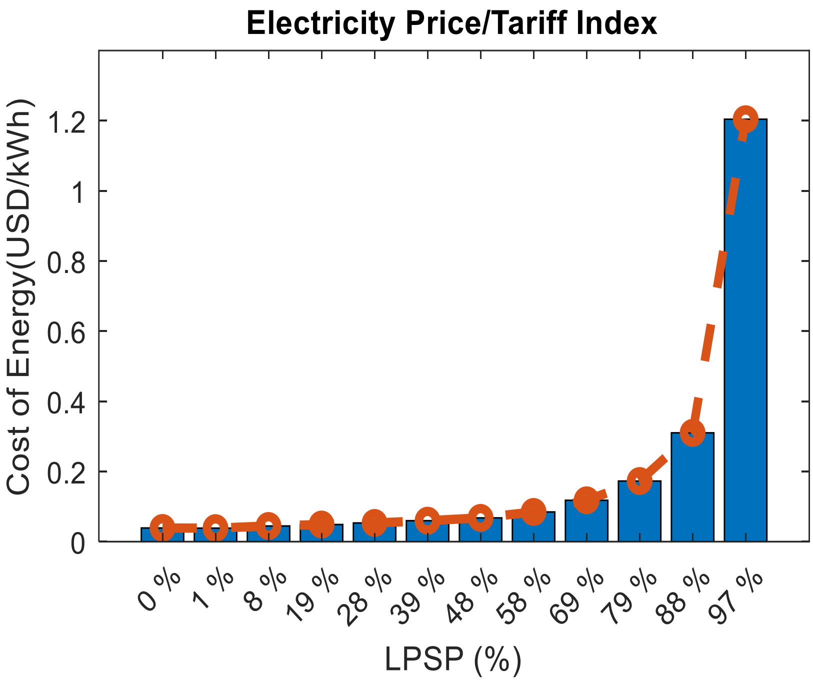

Figure 6: Electricity Price Index (EPI)

Finally, the optimization curve is also shown in Figure 7. It can be observed that the algorithm has faster rate of convergence such that in less than 30% of the iterations the algorithm had already converged.

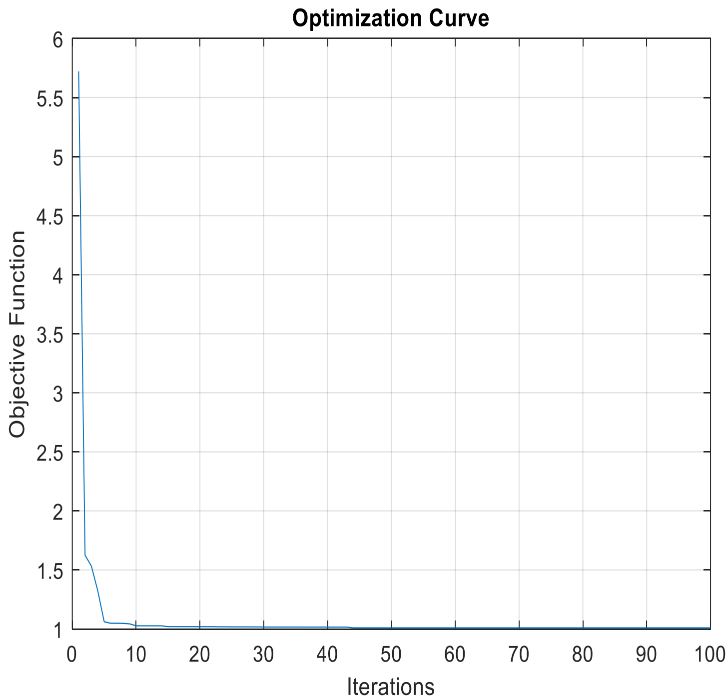

Figure 7: The IGWO Based Hybrid MG Sizing Optimization Curve

Comparative Analysis for Validation of Results

To investigate the accuracy and performance of the IGWO algorithm, an islanded microgrid optimal sizing problem comprising of 4 distinct energy resource configurations was considered (Fathi et. al, 2021) and validation results are given in Table 3. The microgrid configuration includes:

i. DG-FT microgrid system comprising of a fuel tank (FT) coupled with a diesel generator (DG) only.
ii. DG-FT-PV-WT microgrid system comprising of DG-FT, PV and WT system.
iii. DG-FT-PV-WT-BB microgrid system comprising of DG-FT, PV, WT and battery bank (BB).
iv. PV-WT-BB renewable energy system comprising of a PV, WT and BB.

Table 3: Optimal Component Sizing

		DG (kW)	FT (kL)	PV (kW)	WT (kW)	BB (kW)
DG-FT	PSO	700	60	N/A	N/A	N/A
	DE	700	60	N/A	N/A	N/A
	WCA	700	60	N/A	N/A	N/A
	GWO	700	60	N/A	N/A	N/A
	IGWO	**700**	**60**	N/A	N/A	N/A
DG-FT-PV-WT	PSO	700	60	74.9	0	N/A
	DE	700	60	10	10	N/A
	WCA	700	60	74.9	0	N/A
	GWO	700	60	74.9	0	N/A
	IGWO	**700**	**60**	**10**	**10**	N/A
DG-FT-PV-WT-BB	PSO	700	40	385.5	300	891
	DE	700	50	10	250	526.5
	WCA	700	40	333.9	360	607.5
	GWO	700	40	385.5	300	891
	IGWO	**700**	**50**	**10**	**255**	**522.5**
PV-WT-BB	PSO	N/A	N/A	1520.9	470	9450
	DE	N/A	N/A	1665.4	630	8802
	WCA	N/A	N/A	1501.9	490	9612
	GWO	N/A	N/A	1520.9	470	9450
	IGWO	N/A	N/A	**1655.4**	**630**	**8836**

Table 4 presents the NPV values of the overall system obtained via the metaheuristic algorithms over 10 consecutive runs. It was found that, the presence of PV and WT can result in a randomly varying NPV with simulation runs. This may be associated with the uncertain nature of renewable energy resource. In DG-FT system, the NPV was fixed at 8.00 for all runs. However, the addition of renewable resource slightly decreases the NPV while omission of DG results in a higher NPV. The proposed IGWO was able to minimize the NPV lower than some algorithm and as such proved applicable for optimal sizing of HMGS.

Table 4: Comparison of NPV for Different Approaches

Number of Runs		Run 1	Run 2	Run 3	Run 4	Run 5	Run 6	Run 7	Run 8	Run 9	Run 10
DG-FT	PSO	8.00	8.00	8.00	8.00	8.00	8.00	8.00	8.00	8.00	8.00
	DE	8.00	8.00	8.00	8.00	8.00	8.00	8.00	8.00	8.00	8.00
	WCA	8.00	8.00	8.00	8.00	8.00	8.00	8.00	8.00	8.00	8.00
	GWO	8.00	8.00	8.00	8.00	8.00	8.00	8.00	8.00	8.00	8.00
	IGWO	**8.00**	**8.00**	**8.00**	**8.00**	**8.00**	**8.00**	**8.00**	**8.00**	**8.00**	**8.00**
DG-FT-PV-WT	PSO	7.94	7.98	7.94	7.94	7.98	7.94	7.94	7.97	7.94	7.94
	DE	7.98	7.98	7.98	7.98	7.99	7.98	7.99	7.98	7.98	7.98
	WCA	7.94	7.94	7.97	7.94	7.98	7.96	7.98	7.94	7.94	7.96
	GWO	7.94	7.94	7.94	7.94	7.97	7.94	7.96	7.94	7.98	7.94
	IGWO	**7.96**	**7.96**	**7.98**	**7.95**	**7.98**	**7.98**	**7.99**	**7.98**	**7.96**	**7.95**
DG-FT-PV-WT-BB	PSO	6.86	6.95	6.86	6.86	6.88	6.89	6.91	6.86	6.86	6.88
	DE	7.62	7.68	7.72	7.62	7.65	7.66	7.70	7.62	7.63	7.62
	WCA	7.12	7.12	7.18	7.21	7.28	7.12	7.25	7.25	7.12	7.18
	GWO	6.89	6.86	6.86	6.92	6.88	6.86	6.86	6.94	6.86	6.88
	IGWO	**6.87**	**6.87**	**6.89**	**6.95**	**6.99**	**6.86**	**6.96**	**6.98**	**6.86**	**6.92**
PV-WT-BB	PSO	11.68	11.68	11.68	11.70	11.68	11.68	11.68	11.70	11.68	11.70
	DE	12.07	12.09	12.07	12.07	12.07	12.09	12.07	12.14	12.07	12.12
	WCA	11.90	11.84	11.89	11.84	11.86	11.84	11.84	11.84	11.88	11.84
	GWO	11.68	11.68	11.68	11.70	11.68	11.69	11.68	11.68	11.70	11.68
	IGWO	**11.73**	**11.71**	**11.73**	**11.73**	**11.72**	**11.72**	**11.71**	**11.71**	**11.73**	**11.71**

Finally, the developed IGWO was compared with the other existing algorithm in terms of annual operational results with different methods for the system configurations. In general it may be observed in Table 5 that, the higher the uncertainty, the higher the dumped energy supply. The presence of BB system minimizes fuel consumption and gas emission, thereby raising the renewable generation utilization higher than the diesel generation counterpart. Also, it can be observed that the CPU time for IGWOA was relatively lower.

Table 5: Comparison of Energy Production, and Fuel Consumption

		Diesel generation (MWh)	Renewable generation (MWh)	Fuel consumption (kL)	CO_2 emission (tons)	Dumped energy (MWh)
DG-FT	**PSO**	1263.75	N/A	429.68	1164	54.21
	DE	1263.75	N/A	429.68	1164	54.21
	WCA	1263.75	N/A	429.68	1164	54.21
	GWO	1263.75	N/A	429.68	1164	54.21
	IGWO	**1263.75**	N/A	**429.68**	**1164**	**54.21**
DG-FT-PV-WT	**PSO**	1232.24	97.25	418.96	1135	119.95
	DE	1251.13	24.78	425.38	1153	66.37
	WCA	1232.24	97.25	418.96	1135	119.95
	GWO	1232.24	97.25	418.96	1135	119.95
	IGWO	**1232.24**	**97.25**	**418.96**	**1135**	**119.95**
DG-FT-PV-WT -BB	**PSO**	607.57	854.64	206.57	5509.74	232.1
	DE	960.69	308.07	326.64	885.1	51.55
	WCA	677.95	858.46	230.5	624.59	311.76
	GWO	607.57	854.64	206.57	559.74	232.1
	IGWO	**713.45**	**718.95**	**242.57**	**1894.79**	**206.88**
PV-WT -BB	**PSO**	N/A	2529.49	N/A	N/A	1256.16
	DE	N/A	2905.97	N/A	N/A	1637.09
	WCA	N/A	2528.43	N/A	N/A	1255.56
	GWO	N/A	2529.49	N/A	N/A	1256.16
	IGWO	N/A	**2623.35**	N/A	N/A	**1351.24**

Optimization Performance Analysis

The proposed IGWO was further compared with four other existing algorithms including WCA, GWO, DE, and PSO using the NPV optimization curves, LCOE and simulation/CPU time. The graphical description of the performances is presented in Figure 8 through 10. It can be observed from Figures 8 that the developed IGWO was able to minimize the LCOE lower than the other algorithms, and over a relatively shorter computational time as presented in Figure 9. Furthermore, the developed IGWO demonstrated a faster convergence speed (to a global minimum) than its counterparts as may be observed in Figure 10(a) through 10(d).

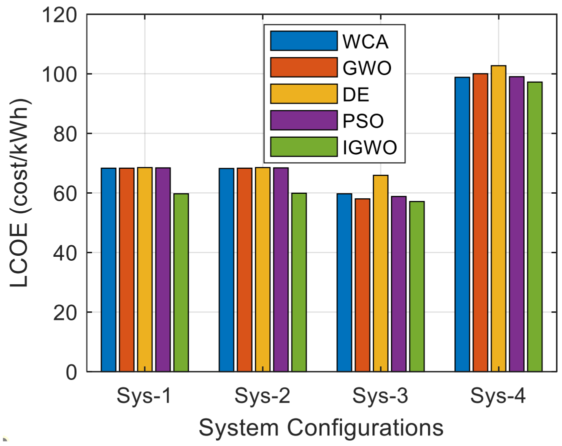

Figure 8: Comparison of LCOE

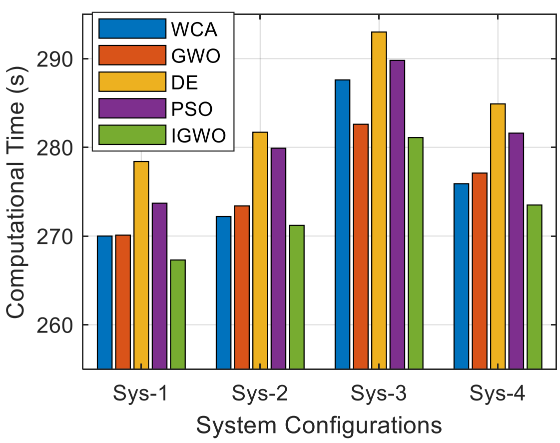

Figure 9: Comparison of Computational Time(s)

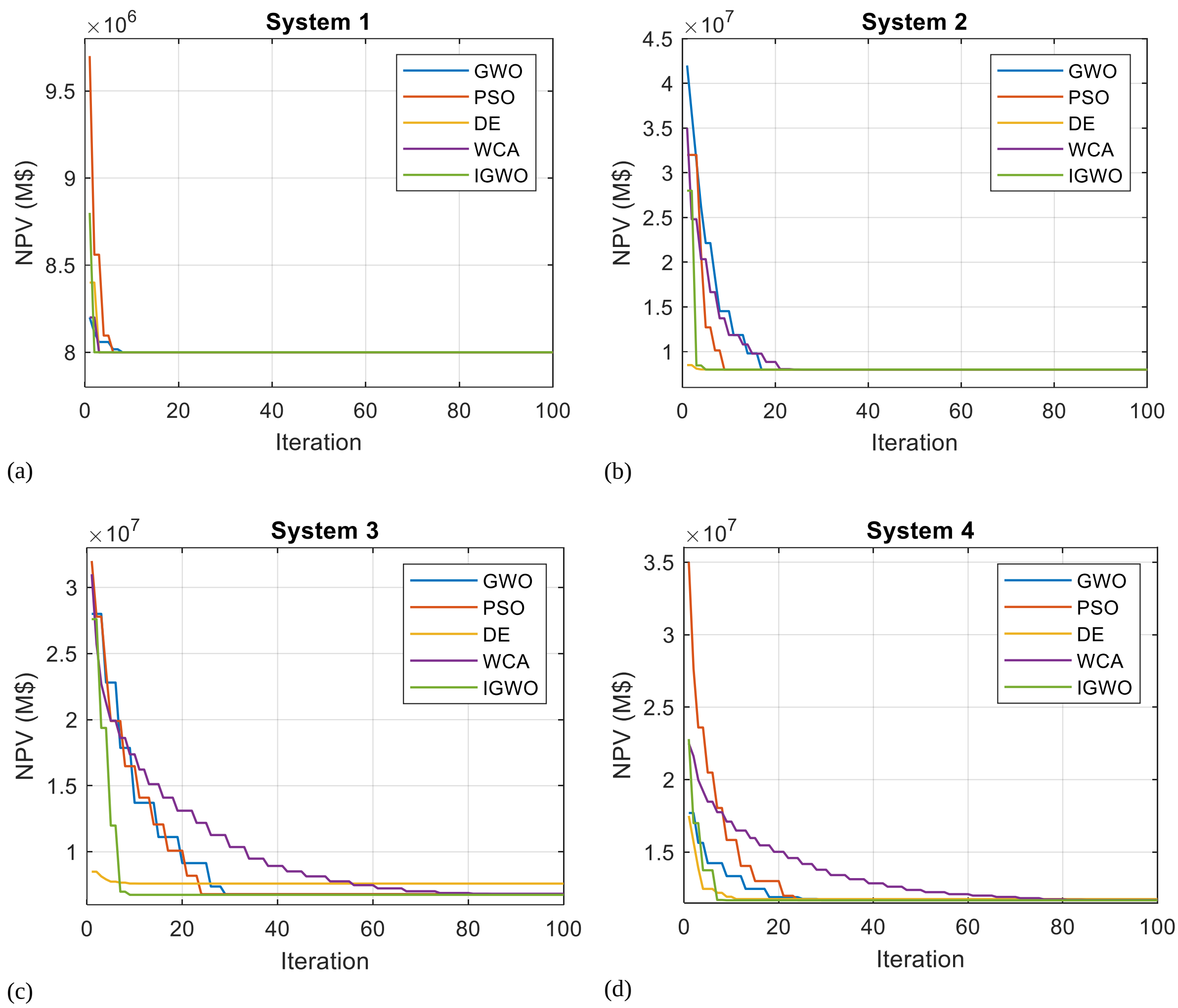

Figure 10: Comparison of NPV, (a) System-1, (b) System-2, (c) System-3, (d) System-4

CONCLUSION

A standalone hybrid microgrid system has been proposed for electricity production in a rural community of Kaduna State in Nigeria. In this work, IGWOA was used in conjunction with four developed models, namely; PV-model, WT-model, LPSP/reliability-model, and BES-model, to carry out an investigative analysis of optimal PV, WT and BES sizing for reliable microgrid operation. The pseudo codes of the aforementioned models have been developed to ease implementation in MATLAB environment. A novel performance index namely, EPI have been introduced to quantify the degree of optimality of the solution. It has also been found that with an investment cost of 162,824 USD per year, the LPSP can be decreased to 0%, whereas a 50% LPSP will result in about 70,411 USD per annum. As such, larger investment cost results in cheaper electricity. The depth of discharge, the charging and discharging efficiency are three main parameters affecting the installed capacity of BES system.

REFERENCES

Administration, U. E. (2016). *International Energy Outlook.* Washington, DC, USA: U.S. Energy Information Administration.

Ainah, P. E. (2015). Development of Microgrid in Sub-Saharan Africa: An overview. *International Review of Electrical Engineering*, Vol. 10, No. 5, pp. 663-645, doi: https://doi.org/10.15866/iree.v10i5.5943

Akinyele, D. E. (2016). Stategy for Developing Energy Systems for Remote Communities: Insights to Best Practices and Sustability. *Sustainable Energy Technologies and Assessment*, *Vol 16*, pp. 106-127, https://doi.org/10.1016/j.seta.2016.05.001

Akram, U., K. Muhammad, & Shafiq, S. (2017). Optimal Sizing of a Wind/Solar/Battery Hybrid Grid-Connected Microgrid System. *IET Renewable Power Generation, Vol. 12, Issue 1*, pp. 72-80, doi: 10.1049/iet-rpg.2017.0010

Bogdanov, D., Ram, M., & Aghahosseini, A. E. (2021). Low-Cost Renewable Electricity as the Key Driver of the Global Energy Transition Towards Sustainability. Energy, Elsevier, Vol. 227(C), pp. 227. doi: 10.1016/j.energy.2021.120467

Dan-Isa, A. & Kadandani, N.B. (2013). Assessment of Wind Energy Potential for Electricity Generation in Katsina, Nigeria. *Bayero Journal of Engineering and Technology (BJET), Vol. 8 No. 2,* pp. 36 – 42, Available Online at: https://bayerojet.com

Enerdata. (2017). *Global Energy Statistic.* https://yearbook.enerdata.net ,kkklll'p/{O>

Fathi, M., Khezri, R. Yazdani, A. & Mahmoudi, A. (2022). Comparative Study of Metaheuristic Algorithms for Optimal Sizing of Standalone Microgrids in a Remote Area Community. *Neural Computing and Applications*. 34(2): pp. 1-19, doi: 10.1007/s00521-021-06165-6.

Jayachandran M., & Ravi, G. (2017). Design and Optimization of Hybrid Micro-Grid System. 1st *International Conference on Power Engineering, Computing and Control, PECCON.* VIT University, Chennai Campus, Energy Procedia 117 (2017) pp. 95–103, doi: 10.1016/j.egypro.2017.05.111

Kadandani, N.B. (2015). Grid Integration of Wind Farms for National Development, - A Case Study of Katsina Metropolis, Nigeria. *Proceedings of North West University Faculty of Science 1st Annual International Conference, Kano, Nigeria*, pp. 380 – 385

Kadandani, N.B., Hassan, S. & Abubakar I. (2023a). Solid State Transformer (SST) and the Challenges of the Future Grid. *FUDMA Journal of Sciences (FJS), Vol. 7 No. 3*, (Special Issue), pp. 330 – 335, doi: https://doi.org/10.33003/fjs-2023-0703-1965

Kadandani, N.B., Hassan, S. & Abubakar I. (2023b). On the Suitability of Modular Multilevel Converter (MMC) in High Voltage Direct Current (HVDC) Transmission System. *FUDMA Journal of Sciences (FJS), Vol. 7 No. 3,* (Special Issue), pp. 318 - 323, doi: https://doi.org/10.33003/fjs-2023-0703-1963

Li, J. W. Wei & Xiang, J. (2012). A Simple Sizing Algorithm for Stand-Alone PV/Wind/Battery Hybrid Microgrids. *Energies*, *Vol. 5*, *Issue 12*, pp. 5307-5323. doi: *https://doi.org/10.3390/en5125307*

Liu, Y., Sun, J, Yu, H. Wang, Y. & Zhou, X.. (2019). *An Improved Grey Wolf Optimizer Based on Differential Evolution and OTSU Algorithm, Applied Sciences, 10(18), 6343;* https://doi.org/10.3390/app10186343

Long, J. C. (2016). Improved Grey Wolf Optimization Algorithm for Constrained Mechanical Design Problems. *Applied Mechanics and Materials*, 851 pp. 553–558. doi: 10.4028/www.scientific.net/AMM.851.553

Mirjalili, S., Mirjalili, S.M. and Lewis, A. (2014) Grey Wolf Optimizer. Advances in Engineering Software, 69, pp. 46-61. doi: http://dx.doi.org/10.1016/j.advengsoft.2013.12.007.

Mousa, K., AlZu'bi, H. & Diabat A. (2010). Design of a Hybrid Solar-Wind Power Plant Using Optimization. *Second International Conference on Engineering System Management and Application (ICESMA 2010), Sharjah, United Arab Emirates,* pp. 1-6, Art. No. 5542695

Varetsky, Y. & Hanzelka, Z. (2015). Modeling Hybrid Renewable Energy System for Micro Grid. *International Conference on Renewable Energies and Power Quality (ICREPQ'15).* La Coruña (Spain), pp. 429-432, doi: https://doi.org/10.24084/repqj13.347

Wang J.S., & Li S.X. (2019) An Improved Grey Wolf Optimizer Based on Differential Evolution and Elimination Mechanism. *Sci Rep.* 2019 May 9;9(1):7181. doi: 10.1038/s41598-019-43546-3. PMID: 31073211; PMCID: PMC6509275.